Atmospheric Research 213 (2018) 17–26

Contents lists available at ScienceDirect

Atmospheric Research

journal homepage: www.elsevier.com/locate/atmosres

Increasing extent and intensity of thunderstorms observed over the Congo Basin from 1982 to 2016

Ajay Raghavendra*, Liming Zhou, Yan Jiang, Wenjian Hua

Department of Atmospheric and Environmental Sciences, University at Albany, State University of New York, Albany, NY, USA

ARTICLE INFO

Keywords:
Africa
Climate change
Congo rainforest
Inter-tropical convergence zone
Satellite IR brightness temperature
And tropical convection/thunderstorms

ABSTRACT

Recent studies found a long-term drought and resulting declines in vegetation greenness and canopy water content over the Congo Basin, the second largest rainforest in the world after the Amazon. Since most precipitation in tropical latitudes stems from convection, this paper analyzed 35 years of high-resolution (8 km spatial resolution and 3 h temporal resolution) satellite data to document the long-term trends in the number, size and intensity of thunderstorms activity over the Congo Basin during April, May, and June (AMJ) for the period 1982–2016. Changes in the magnitude and area of cold cloud top brightness temperatures (T_b) at different thresholds were used as a proxy to quantify the number and size of individual thunderstorms at different intensities. We found that the areal extent and intensity of thunderstorms increased over the past 35 years, particularly over Northern Congo Basin, and these changes are consistent with other satellite datasets. Combined with a reanalysis dataset, our work suggests that thunderstorms over the Congo Basin are becoming taller and wider, and likely resulting in a moister (drier) upper (lower) troposphere.

1. Introduction

Central Africa is one of the most convective regions characterized by intense thunderstorm activity (Zipser et al., 2006). As thunderstorms are convective systems accompanied by the occurrence of lightning, Democratic Republic of Congo in Central Africa is known as the thunderstorm and lightning capital of the world (Cecil et al., 2015). Because most of the accumulated rainfall in tropical latitudes originates from convective type precipitation (Dai, 2006), large changes in atmospheric convection activities are expected to have significant impacts on rainfall patterns over this region. Understanding such changes could provide insights into observed variations in rainfall characteristics and future rainfall trends in a warming climate over Africa, one of the most vulnerable continents to climate change and climate variability (Niang et al., 2014; Maidment et al., 2015).

Recent studies (Malhi and Wright, 2004; Asefi-Najafabady and Saatchi, 2013; Zhou et al., 2014; Hua et al., 2016, 2018) have identified a long-term drying trend in Central Africa, particularly over the Congo Basin (hereafter *Congo*). This drought may have a negative impact on the Congolese rainforest, the second largest rainforest in the world after the Amazon. Zhou et al. (2014) found a large-scale decline in vegetation greenness and canopy water content over the intact Congolese rainforest for the period 1988–2012 using multiple satellite datasets and attributed this decline to the long-term drought. Guan et al. (2015) and Harris et al. (2017) also found losses in forest productivity and vegetation cover over the Congo. These changes have important implications as tropical rainforests function as the global biodiversity hotspots and influence local, regional, and global weather and climate systems through various biogeochemical and biogeophysical processes (e.g., Lewis, 2006; Lewis et al., 2009; Pokam et al., 2012).

Possible physical mechanisms responsible for this drying trend over the Congo were explored by Hua et al. (2016, 2018). Based on analyses of multiple reanalysis datasets, and climate modeling experiments, Hua et al. (2016, 2018) linked the drying trend to tropical sea surface temperature (SST) anomalies and associated changes in the tropical Walker circulation. While a significant relationship between the anomalies in the Congo precipitation and large-scale atmospheric circulation was identified, we do not fully understand how convection, which is responsible to generating the majority of precipitation in tropical latitudes (Dai, 2006), has changed over the Congo. Furthermore, it is difficult to study precipitation and thunderstorm trends using coarse resolution data (e.g., reanalysis, weather, and climate models) given their inability to accurately capture the diurnal cycle, frequency, and rain rate when compared to observations (Dai, 2006). Therefore, satellite datasets are perhaps the best and most reliable observational platforms to study thunderstorms and convection over Central Africa.

Satellite products have been used to understand convection over Central Africa. Hodges and Thorncroft (1997) presented a short 8-year

* Corresponding author at: Earth Sciences 330, University at Albany, 1400 Washington Ave., Albany, NY 12222, USA.
E-mail address: araghavendra@albany.edu (A. Raghavendra).

https://doi.org/10.1016/j.atmosres.2018.05.028
Received 12 February 2018; Received in revised form 17 May 2018; Accepted 27 May 2018
Available online 30 May 2018
0169-8095/

satellite-derived storm track and thunderstorm climatology for Africa, and Futyan and Del Genio (2007) examined convection and storm tracks over the tropical Atlantic Ocean and Africa using four months of satellite data. Several studies (e.g., Laing and Fritsch, 1993; Petersen and Rutledge, 2001; Yang and Slingo, 2001) explored mesoscale convective system (MCS) activity, atmospheric convection, and precipitation over Africa using satellite data over a period of 2–4 years. However, a comprehensive satellite-based climatology and variability of convection activity over the Congo do not exist. In more recent years, Taylor et al. (2017) found a tripling in thunderstorm activity and a proportionally large increase in rainfall during the months of June, July, and August (JJA) over the Sahel using satellite data, but paid little attention to the Congo. This implies that the changes in the number, intensity, and size of thunderstorm activity over the Congo have not been documented nor well understood. Motivated by this knowledge vacuum, here we seek to shed light on the long-term trends in convection over the Congo by using 35-years of high-resolution satellite data.

The paper is organized as follows. Section 2 provides a brief description of datasets and methods used. Results pertaining to the long-term trends in the number, intensity, and size of thunderstorms are presented in Section 3. Major conclusions and possible physical mechanisms are discussed in Section 4.

2. Data and methods

2.1. Satellite datasets

We used the gridded infrared (IR) channel brightness temperature T_b dataset (GridSat-B1; Knapp, 2008; Knapp et al., 2011) sampled by the European Meteosat (MET) series of geostationary satellites (MET 2–10; Table 1) for 35 years (1982–2016). GridSat-B1 obtained the data from the International Satellite Cloud Climatology Project (ISCCP; Schiffer and Rossow, 1983), mapped them on a 0.07-degree latitude equal-angle grid at a 3-h temporal resolution, and applied a view zenith angle correction (Joyce et al., 2001). It contained the data for visible (VIS; 0.7μm), IR (11.0μm), and water vapor (WV; 7.7μm) channels, but only the IR window channel data was used since the other channels were not considered to be of Climate Data Record (CDR) program quality (National Research Council (NRC), 2004). While the frequency of missing data is relatively higher from 1982 to 1985 when compared to the long-term record, we alleviated issues pertaining to missing data by calculating the mean thunderstorm activity by season (i.e., AMJ which consist of 91 days).

2.2. Other datasets

It is impossible to study thunderstorms or MCSs given the relatively poor spatio-temporal resolutions of most datasets (e.g., global reanalyses). However, it may be possible to trace significant changes observed in the mesoscale activities (e.g., thunderstorms) projecting on to, and influencing some variables in the larger scale circulation and dynamics. Here we examined outgoing longwave radiation (OLR), vertical motion (vertical velocity '*w*'), and moisture fields (specific humidity 'q') using three different datasets:

- European Centre for Medium-Range Weather Forecast (ECMWF) interim reanalysis (ERA-Interim; Dee et al., 2011)
- National Oceanic and Atmospheric Administration (NOAA) OLR–Daily CDR (Lee et al., 2014)
- NOAA's Interpolated OLR (Liebmann and Smith, 1996).

It is important to note that the GridSat-B1 dataset was obtained from geostationary satellites whereas the two NOAA's OLR datasets were produced from polar orbiting satellites. In addition, the T_b dataset from the CLoud Archive User Service (CLAUS; Hodges et al., 2000) was also used. In this study, an intercomparison between four different satellite derived products (i.e., two T_b datasets from GridSat-B1 and CLAUS, and two OLR data datasets from NOAA) was carried out to ensure confidence in the major results presented in the paper using the GridSat-B1 T_b dataset.

Table 1
A list of geostationary satellites used from 1982–present that were used to provide coverage over the Congo basin (adapted from NOAA's ISCCP B1 Satellite Information webpage available at https://www.ncdc.noaa.gov/gridsat/index.php).

Satellite	Launch date	Period of record	
		From	To
MET-02	19-Jun-1981	31-Aug-1983	24-Aug-1988
MET-03	15-Jun-1988	24-Aug-1988	19-Jun-1989
MET-04	06-Mar-1989	19-Jun-1989	04-Feb-1994
MET-05	02-Mar-1991	01-Jan-1994	01-Feb-1997
MET-06	20-Nov-1993	12-Feb-1997	20-Jan-2000
MET-07	02-Sep-1997	31-May-1998	01-Jan-2005
MET-08	28-Jul-2002	01-Jan-2005	10-May-2007
MET-09	21-Dec-2005	10-May-2007	20-Jan-2013
MET-10	05-Jul-2012	20-Jan-2013	present

2.3. Methods

Our study region is limited to the Congo rainforest that lies on the Equator, defined as the area enclosed by 8°N–8°S and 12.5°E–32.5°E (1778 km × 2222 km near equator), and covers an area of approximately 3.9 million km^2. This constitutes a total of 65,208 pixels in the GridSat-B1 dataset. The Congo rainforest has a complicated seasonality of precipitation that is closely linked with the seasonal passage of the *rainbelt* that migrates *north* and *south* across the equator throughout the course of the year (e.g., Nicholson, 2014). The causal factors governing the characteristics of the rainfall regime and its interannual variability, including atmospheric circulation, sea surface temperature, moisture flux, and convective activity, differ markedly by season within equatorial Africa and the Congo Basin (e.g., Dezfuli and Nicholson, 2013; Nicholson and Dezfuli, 2013; Nicholson, 2014). These factors can interact nonlinearly to enhance and weaken their individual contributions at different months and seasons, making it difficult to detect long-term climate signals. To minimize seasonal variations of such interactions, here we focus on the three-month period of April, May, and June (AMJ) given the strong seasonality in moisture source (Dyer et al., 2017) and precipitation over the Congo (Washington et al., 2013), and to effectively compare our results to existing literature where a strong drying trend was documented during AMJ (e.g., Zhou et al., 2014; Hua et al., 2016, 2018). Although AMJ represents the transition period from precipitation maxima in April to drier conditions in June (Washington et al., 2013), it corresponds to one of two peak growing seasons for the rainforests.

It is crucial to note that the equator passes through the Congo. This implies that the tropical diurnal and season cycles strongly influence convection and precipitation over the Congo. The tropical diurnal cycle (e.g., Yang and Slingo, 2001) plays an important role in regulating convection over our study region. The diurnal cycle observed in the GridSat-B1 dataset (not shown) was quite typical for convection over land in tropical latitudes i.e., peak in convective activity observed around 15–18 local standard time (LST; e.g., Yang and Slingo, 2001; Nesbitt and Zipser, 2003). Also, our analysis does not filter for the time of peak convection activity (e.g., 1800LST in Taylor et al., 2017) since we are able to document significant trends in thunderstorm activity using data from all times of the day.

T_b has been used as an alternate to radiance to detect clouds and

quantify cloud top temperatures (Schmetz et al., 1997). Thermal infrared radiation in the atmospheric window is very sensitive to both surface temperature and cloud cover, especially deep convective clouds (thunderstorms). Over tropical rainforests, the diurnal and seasonal variations in surface temperature are much smaller than other ecosystems (e.g., Mildrexler et al., 2011), but the presence of convective clouds will largely modify the satellite measured radiance due to the pronounced contrast of temperatures between warm surfaces and very cold cloud tops. Different T_b thresholds are often used to measure deep convective clouds and quantify thunderstorm systems: the deeper the convection, the stronger the intensity, and the lower the T_b value. In other word, changes in the magnitude and area of very low T_b at different thresholds can be used as a proxy to quantify the number and size of thunderstorms at different intensities (e.g., Maidment et al., 2014).

The MET satellites are centered along the prime meridian and provide excellent coverage over Central Africa, which includes our domain of interest. The GridSat-B1 dataset has the best inter-calibrated IR window channel and is well-suited for analyzing the horizontal structure of thunderstorms over the Congo (Knapp, 2012). For illustrative purposes, an image from the Global ISCCP B1 Browse System (GIBBS; available online at https://www.ncdc.noaa.gov/gibbs/) archive was obtained to provide an example of IR T_b associated with thunderstorms over the Congo (Fig. 1a). In Fig. 1a we observed a line of convection in the eastern part of the domain, and a cluster of thunderstorms near the middle of the domain. Some intense convection characterized by very low T_b (i.e., $T_b < -60^{\circ}C$) was present over Sudan and Chad (north east with respect to our study region).

At each three-hourly time step, the gridded IR T_b data over the study region was obtained and contours of T_b less than or equal to a given prescribed T_b threshold were drawn. Fig. 1b presents a thunderstorm cell in an idealized framework to help illustrate the vertical structure of individual convective towers. An enclosed contour represents a thunderstorm cell for a given T_b threshold and some deep convective thunderstorms may overlap with shallow convective systems at different T_b thresholds. For instance, the contour C-1 in Fig. 1b depicted in black delineates lowest clouds with highest T_b, but it also includes the middle cloud contours C-2 (blue) and C-3 (orange) with intermediate T_b and the high cloud contour C-3 in red with lowest T_b. The number of thunderstorms, the mean size (or area) of each thunderstorm, and the mean T_b value (or intensity) of each thunderstorm were documented by searching for the contours containing a specified T_b threshold and drawing T_b contours of temperatures less than or equal to the prescribed T_b threshold. While T_b based contours were drawn using multiple T_b thresholds, for the sake of clarity and to avoid cluttering the figures only the results from the thresholds of $-40^{\circ}C$, $-50^{\circ}C$, $-60^{\circ}C$, and $-70^{\circ}C$ T_b are shown in this paper. The -40 to $-70^{\circ}C$ temperature range is representative of thunderstorms and deep convection in tropical latitudes (e.g., Taylor et al., 2017). This procedure helped us obtain the total number of thunderstorms, and the mean size and intensity of individual thunderstorm cells at four different T_b thresholds over the study region eight times per day. We also validated the correctness of our computing algorithm by independently verifying the findings of Taylor et al. (2017) and found a similar tripling in MCS activity over the Sahel.

Finally, linear trend analysis based on least squares regression was employed to quantify long-term changes in thunderstorm characteristics (i.e., number, size, and total areal extent) in the GridSat-B1 dataset at both the grid and regional level. Linear trend analysis was also used to document changes in OLR, vertical velocity, and moisture from other coarser resolution datasets. The statistical significance level or the P value, is estimated by the two-tailed student's test to quantify whether the trend is statistically significant rather than an artifact of random noise.

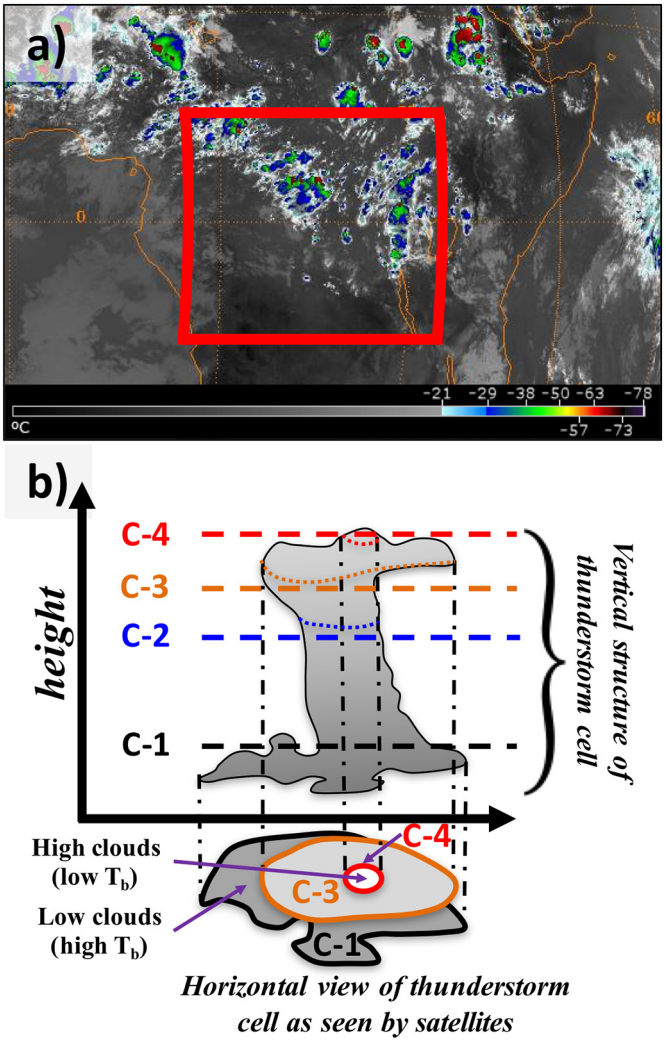

Fig. 1. a) An example of a satellite image obtained by Meteosat–7 on 1500 UTC 9 August 2015 and made available via GIBBS. The domain of interest in this study is depicted using a red box. b) An idealized thunderstorm cell showing clouds contoured at different T_b. C-1, C-2, C-3, and C-4 represent different temperature thresholds at which contours were drawn. (For interpretation of the references to colour in this figure legend, the reader is referred to the web version of this article.)

3. Results

3.1. Areal extent and intensity of thunderstorm

Understanding trends in the total number of pixels across different T_b thresholds acted as a primer and provided motivation to further explore thunderstorm activity over the Congo. This was achieved by simply counting the number of pixels satisfying the T_b thresholds range for each image and then calculating the mean by season. From Fig. 2a, we observed a significant increase of 3.4–1.4 pixels yr^{-1} ($p < 0.01$) in the mean pixel count across four relatively very cold T_b ranges, i.e., $-85^{\circ}C$ to $-70^{\circ}C$, likely attributed to an increase in intense thunderstorm activity. Notwithstanding variability in the interannual timescale, this serves as direct evidence that the areal extent of very cold T_b corresponding to thunderstorms have increasing for the past 35 years. Fig. 2a also showcases the MET series satellites used over the Congo to construct the long-term record (Table 1) in the figure background. This helps us to easily identify any sharp changes in pixel count and changes in satellites used in constructing the dataset. There is no evidence to suggest that the trends obtained from the GridSat-B1 dataset are an

artifact of changes in satellites across the 35-year study period (e.g., Maidment et al., 2014). Further, the dataset has already been calibrated and verified by Knapp (2008, 2012). Fig. 2b shows a steady decrease of 0.018–0.032$^{\circ}C$ yr^{-1} ($p < 0.01$) in the mean cold cloud top T_b across a relatively large range of cold T_b thresholds, i.e., $-70^{\circ}C$ to $-40^{\circ}C$, indicating that the mean intensity (height) of thunderstorm has increased. This panel was generated by calculating the mean of the mean T_b within each T_b threshold contour for each image and then calculating the mean by season.

3.2. Total number and mean size of thunderstorms

The above results show that the presence of cold cloud top T_b has increased. Next we investigated if this increase was attributed to an increase in the thunderstorm number, and/or thunderstorm size. AMJ is a transitioning season characterized by a precipitation maximum during April and a minimum around June. Also, there lies strong evidence to suggest intensification of thunderstorms towards Northern Congo (Fig. 3) where the mean position of the inter-tropical convergence zone (ITCZ[1]) is also collocated during AMJ. Since we choose to analyze a transitioning season for precipitation (i.e., AMJ) over the Congo, the volume of convection closely followed the predominant position of the ITCZ (Fig. 4). Furthermore, opposite trends were observed in the spatial pattern of temperature over the Northern and Southern Congo (Fig. 4; more details in Section 3.3), we quantify the trends in the number, mean size, and total area of thunderstorms for four different T_b thresholds separately over Northern and Southern halves of the Congo (Fig. 3).

The mean number of thunderstorms significantly increased (39–21% change; $p < 0.1$) across all four T_b thresholds throughout our study region and Northern Congo accounted for > 55% of the observed increase (Fig. 3a–b). While the difference in the number of individual thunderstorm cells between Northern and Southern Congo was relatively small, thunderstorms over Northern Congo appear to be on average 1.2–1.5 times larger when compared to ones over Southern Congo across the four T_b thresholds (Fig. 3c–d). Such regional differences in the observed characteristics and trends in thunderstorms are likely a consequence of a narrowing ITCZ (e.g., Byrne and Schneider, 2016) resulting in more intense and robust thunderstorm activity over Northern Congo than Southern Congo.

Fig. 3c–d shows trends in the mean size (or area) of individual thunderstorm cells per image for four T_b thresholds. This panel shows a decrease at the rate of approximately 9–24 km^{2}yr^{-1} in the mean areal extent of thunderstorm size contoured at $-40^{\circ}C$ and $-50^{\circ}C$, and an increase of 9–29 km^{2}yr^{-1} contoured at $-60^{\circ}C$ and $-70^{\circ}C$. While the number of thunderstorms has increased at all T_b, the mean area of thunderstorms shows a relatively weak decreasing trend at higher T_b ($-40^{\circ}C$ and $-50^{\circ}C$) and an increasing trend at lower T_b ($-60^{\circ}C$ and $-70^{\circ}C$). The viewing angle of the satellite which is perpendicular to the surface results in lower clouds being shadowed by higher clouds (e.g., contour C-2 in Fig. 1b). Therefore, it was difficult to conclude if the horizontal extents of thunderstorm cells have physically decreased at higher T_b(i. e., $-40^{\circ}C$ to $-50^{\circ}C$). We are confident in the increasing trend in the mean areal extent of thunderstorm tops at lower T_b(i. e., $-60^{\circ}C$ to $-70^{\circ}C$). Since the mean cold cloud top T_b has also been steadily decreased and resulting in lower T_b (Fig. 2b), we can conclude with reasonable confidence that thunderstorms have increased in size (i.e., both the width and height of thunderstorms have increased) for the past 35 years. This upward trend may be attributed to an increasing trend in the number density of thunderstorms over the Congo (Fig. 3a–b) that may favor convection aggregation (Muller and Bony, 2015), and intensity of thunderstorms (Fig. 2).

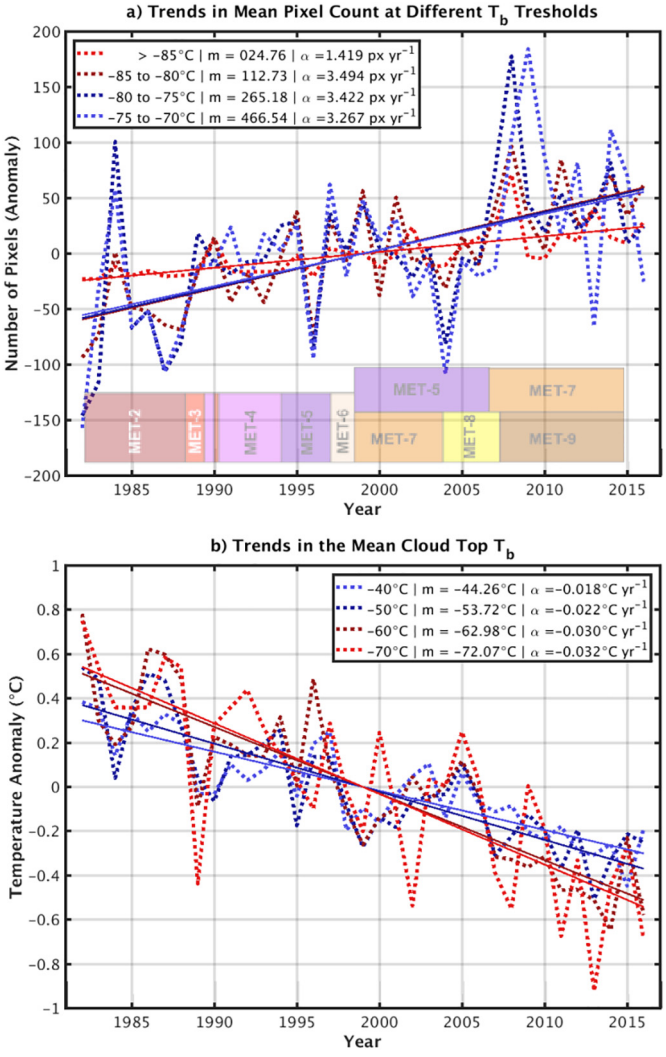

Fig. 2. a) Interannual variations in the AMJ mean pixel count for thunderstorm defined based on four different T_b threshold ranges for the period 1982–2016 over the Congo. As a reference, an illustration of the satellites used over the study region (Table 1) is shown in the background. b) Interannual variations in the mean T_b of thunderstorm cloud tops at four different T_b thresholds. The climatological mean temperature (m) and the linear trend (∝) are shown in the box for each panel. All the trends in both panels are statistically significant at $p < 0.01$.

These results indicate that the number of thunderstorm cells has increased over the Congo and the mean areal extent of thunderstorms at higher (lower) T_b has decreased (increased). However, the total areal extent at different T_b thresholds attributed to the combined effects of the change in number and size of thunderstorms was unanswered. Since trends in the number of thunderstorms were stronger when compared to the mean area of thunderstorms at all four T_b thresholds, it was found that the total areal extent of thunderstorm cloud cover (i.e., multiplying the mean number and mean area of thunderstorms i.e., Fig. 3a–b with Fig. 3c–d) increased (significantly at $-60^{\circ}C$ and $-70^{\circ}C$) at all T_b thresholds (Fig. 3e–f). This increase was stronger over Northern Congo than its Southern counterpart. In fact, no significant trends in the total areal extent of thunderstorm cloud cover were found over Southern Congo at −40 and $-50^{\circ}C$ T_b thresholds (Fig. 3f).

[1] *While it may be technically incorrect to refer to the equatorial convergence zone (ECZ) over Africa as an ITCZ (Nicholson et al., 2018), the term ITCZ will be used in this manuscript to describe the seasonal mean location of peak convection activity.*

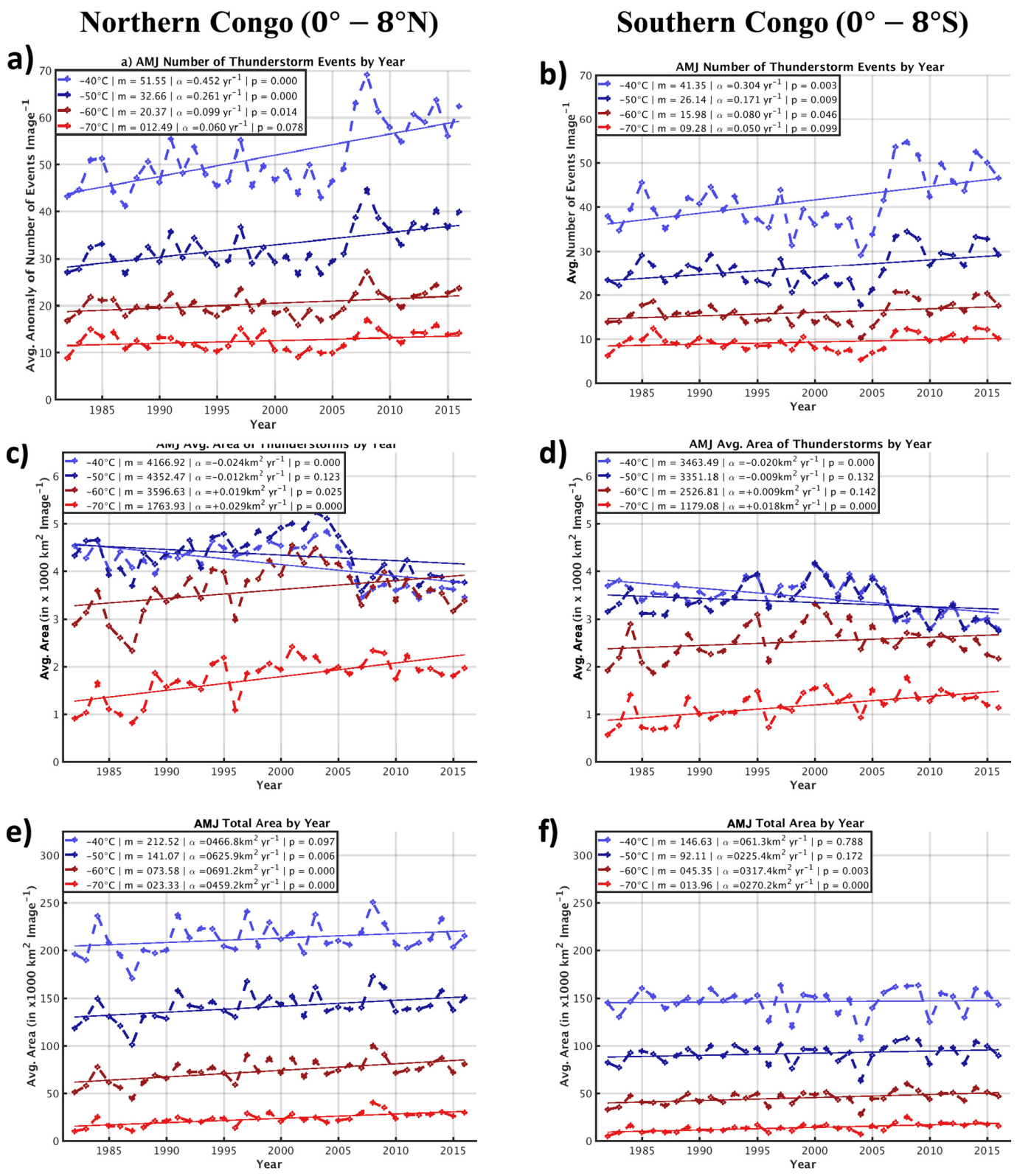

Fig. 3. Interannual variations in the number (top), mean size (middle), and total area (top; i.e., number × mean size) of thunderstorms over Northern Congo (left columns) and Southern Congo (right columns) for the period 1982–2016 during AMJ. The mean (m) and the linear trend (∝), and the *p*-value (p) of the trend are shown in the box for each panel.

3.3. Consistency with other coarser resolution datasets

We found agreement in the AMJ spatial trends among the GridSat-B1 T_b, CLAUS T_b, and the two NOAA's OLR datasets for the common period ranging from 1984 to 2009 (see Fig. 4 and Table 2). All four datasets show orographic enhancement of thunderstorm activity over eastern Congo (e.g., Soula et al., 2016), and similar spatial features in both the seasonal mean and trend. Consistent with the propagation of

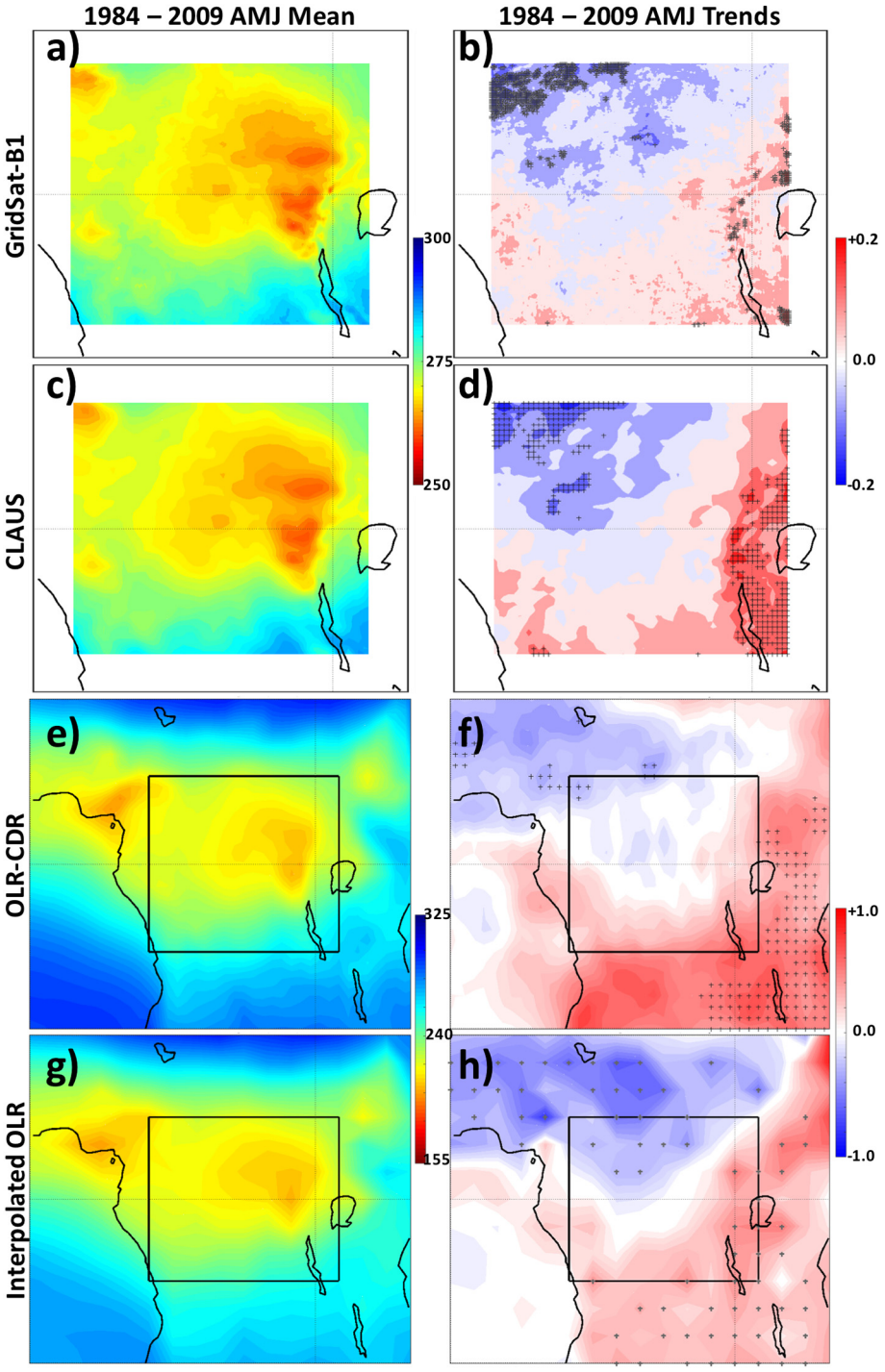

Fig. 4. Spatial patterns of the mean (left columns) and trends (right columns) in T_b (top two rows in K and Kyr^{-1}) and OLR (bottom two rows in Wm^{-2} and $Wm^{-2}yr^{-1}$) from 1984 to 2009 during AMJ. Trends significant at $p < 0.05$ are shown using the '+' symbol.

Table 2
A list of satellite datasets used in this study with the corresponding reference, spatio-temporal resolution, and data availability.

Dataset and reference	Spatial resolution	Temporal resolution	Observation platform	Time range
Geostationary IR channel brightness Temperature - GridSat B1 (Knapp et al., 2011)	0.07°	3 hourly	Geostationary satellite	+36 years (1982–present)
IR T_b from CLoud archive user service (CLAUS) by Hodges et al. (2000)	0.33°	3 hourly	Geostationary satellite	26 years (01 JUL 1983 to 30 JUN 2009)
NOAA OLR–daily CDR PSD interpolated version (Lee et al., 2014)	1.00°	Daily mean	Polar Orbiting satellites	+34 years (1979–2012)
NOAA interpolated OLR by Liebmann and Smith (1996)	2.50°	Daily mean	Polar Orbiting satellites	+44 years (1974–2017)

the ITCZ, thunderstorm activity was concentrated within Northern Congo along with contrasting trends in T_b between Northern and Southern Congo (Fig. 4) i.e., during AMJ, we observe a cooling (warming) Northern (Southern) Congo in the two T_b data sets. The observed consistency among the four satellite datasets, together with our independent verification of results from another paper (i.e., Taylor et al., 2017), bolstered the confidence in the results (i.e., Sections 3.1 and 3.2) using the GridSat-B1 T_b dataset.

The spatio-temporal resolution of thunderstorms that mostly operates in the mesoscale makes it nearly impossible to capture or reproduce thunderstorms in relatively lower resolution reanalysis datasets. However, given the significant long-term trends in thunderstorm activity over the Congo, we were curious in examining long-term trends in OLR, atmospheric dynamic (e.g., vertical motion and moisture fields). We hypothesize that the robust trends observed in thunderstorm activity at the mesoscale could potentially be projected onto the coarser resolution datasets. A decreasing trend in OLR can be attributed to an increasing trend in thunderstorm intensity (or the magnitude of very low cloud top Tb), and/or an increase in the spatial extent of thunderstorms. As expected, the OLR dataset reveled an overall decreasing (increasing) trend over Northern (Southern) Congo (Fig. 5a). Consistent with the findings from Fig. 4e where an increase in the mean areal extent of cold clouds top T_b were observed over Northern Congo, the spatial mean for OLR decreased significantly ($p < 0.02$) over Northern Congo. Analyzing trends in the number of pixels corresponding to tropical convection (i.e., pixels with value < 200 Wm^{-2}) yielded a significant ($p < 0.02$) increasing trend (Fig. 5b). Consistent with the findings from Fig. 4f where relatively weak and insignificant trends were documented in the net areal extent of thunderstorms over Southern Congo, the OLR trends over Southern Congo were weak and mostly insignificant (Fig. 5c).

3.4. Changes in larger scale circulation and dynamics

A somewhat puzzling finding but consistent with previous research (e.g., Kawase et al., 2010; Hua et al., 2016, 2018) was a trend towards weaker ascent ($\partial\omega/\partial t > 0$, i.e., sinking tendency. Note that ω is the vertical pressure tendency in the atmosphere) observed both in the upper and lower troposphere diagnosed using the reanalysis datasets (Fig. 6a and c). The increase in subsidence over a broad area can likely be attributed to local mass conservation to offset the increase in the number of thunderstorm cells (convective towers) observed over the Congo. While a region characterized by weaker ascent is usually associated with a drying trend, we only found a drying trend in the lower troposphere (e.g., Fu, 2015). Trends in specific humidity from the reanalysis dataset are in agreement with other studies that show moistening in the upper troposphere (Fig. 6b; e.g., Soden et al., 2005), and drying in the lower troposphere (Fig. 6d; e.g., Schroeder and McGuirk, 1998). This would imply that the taller and wider thunderstorms, which have increased in number, are likely depositing moisture in the upper troposphere despite an increasing trend towards weaker upward vertical motion. This vertical transport of moisture, decreasing surface precipitation trend, and relatively high-water recycling ratio in the Congo (Dyer et al., 2017) are most likely resulting in a net drying trend in the tropical air mass over the Congo.

4. Conclusions and remarks

This study documented the changes in the number, size and intensity of thunderstorms activity over the Congo during AMJ using 35 years of high resolution satellite T_b data from GridSat-B1. To bolster the confidence in and validate our results, we also analyzed three other coarse resolution satellite datasets and found good agreement among the four datasets (Fig. 4). Our results indicate an increasing trend in the number of thunderstorms, and an increasing (decreasing) trend in the mean thunderstorms area at lower (higher) T_b thresholds over the Congo. We found opposite trends in the volume of thunderstorm activity i.e., increase (decrease) in Northern (Southern) Congo. Given the predominant location of the ITCZ during AMJ (i.e., norther tropical latitudes), over 55% of thunderstorm cells were documented in Northern Congo. While the overall trends in the number and total area of thunderstorms over the Congo show an increase for AMJ, the signal was stronger over Northern Congo (Fig. 3–5). At the same time, our work also suggests that thunderstorms have intensified resulting in taller and wider thunderstorm cells (Figs. 2b and 3c–d). The trends in OLR concurred that the trends in cold top clouds have increased from 1982 to 2017 (Fig. 5).

We would typically associate an increasing trend in thunderstorm activity to an increasing trend towards stronger vertical ascent (i.e., $\partial\omega/\partial t < 0$). However, in a likely response to offset the increase in thunderstorm activity and to conserve mass, large-scale trends favoring weaker ascent were ubiquitous across the vertical column of the atmosphere over the Congo (Fig. 6a and c). Consistent with taller thunderstorms and resulting increase in the spatial extent of cold cloud tops, it was found that the moisture content in the upper troposphere has increased (Fig. 6b; e.g., Soden et al., 2005). A decline in the moisture content in the lower troposphere was also documented (Fig. 6d; e.g., Schroeder and McGuirk, 1998). Fig. 7 presents a schematic representation of the key findings in this study and other relevant research work, i.e., an increase in the number of thunderstorms, an increase in the mean areal extent of thunderstorm cold cloud tops, trends towards weaker ascent across all layers of the atmosphere, moistening (drying) trend in the upper (lower) troposphere, and decreasing trend in soil moisture (Jiang et al., 2018).

The seasonality of the precipitation over the Congo is strongly linked to the poleward seasonal migration of the ITCZ (Washington et al., 2013), and studies such as Su et al. (2017), Byrne and Schneider (2016), and Fu (2015) have found the ITCZ to be narrower and strengthening in a warming climate, and explored variables governing the width of the ITCZ. Going forward, understanding changes in the ITCZ when subjected to changes in its aspect ratio and strength (e.g., Raghavendra and Guinn 2016), and tropical wave activity (e.g., Hung et al. 2013) may help us better explain climate variability and trends in tropical convection and precipitation. While physical mechanisms responsible for the observed trends in thunderstorms over the Congo is beyond the scope of this paper, fundamental knowledge pertaining to the trends in the number and areal extent of thunderstorms was presented. Our results show that the changes in the characteristics of thunderstorms over the Congo have probably caused moisture being transported deeper into the upper troposphere resulting in lesser moisture available to rain down to the surface. It can also be argued that the increased drying trend noted in the lower troposphere (Fig. 6d; McCollum et al., 2000) may restrict raindrops from reaching the surface due to an increase in virga (Sassen and Krueger, 1993). Furthermore, given the high recycling ratio of water over the Congo (e.g., Pokam et al., 2012; Dyer et al., 2017), even a slight decrease in surface precipitation attributed to the redistribution of moisture (for instance to the upper troposphere, or virga) can potentially have a significant impact on the water cycle and vegetation over the Congo.

One of the motivations for this work was linked to the long-term declining trend in rainfall over the Congo (e.g., Zhou et al., 2014; Hua et al., 2016) and subsequent browning of vegetation (Zhou et al., 2014). Since precipitation over tropical latitudes is strongly tied to convection, we found it worthwhile to study trends in thunderstorms with the hope of understanding surface precipitation trends over the Congo. The research work presented in this paper along with other similar works (e.g., Taylor et al., 2017) have found increased thunderstorm activities over the Congo. The increase in thunderstorm intensity, number, and area can possibly be explained by a narrowing and strengthening of the ITCZ coupled with the expanding of the Hadley cell (Byrne and Schneider, 2016). Since a strengthening ITCZ is characterized by stronger updrafts (i.e., strong upward vertical motion), a thunderstorm

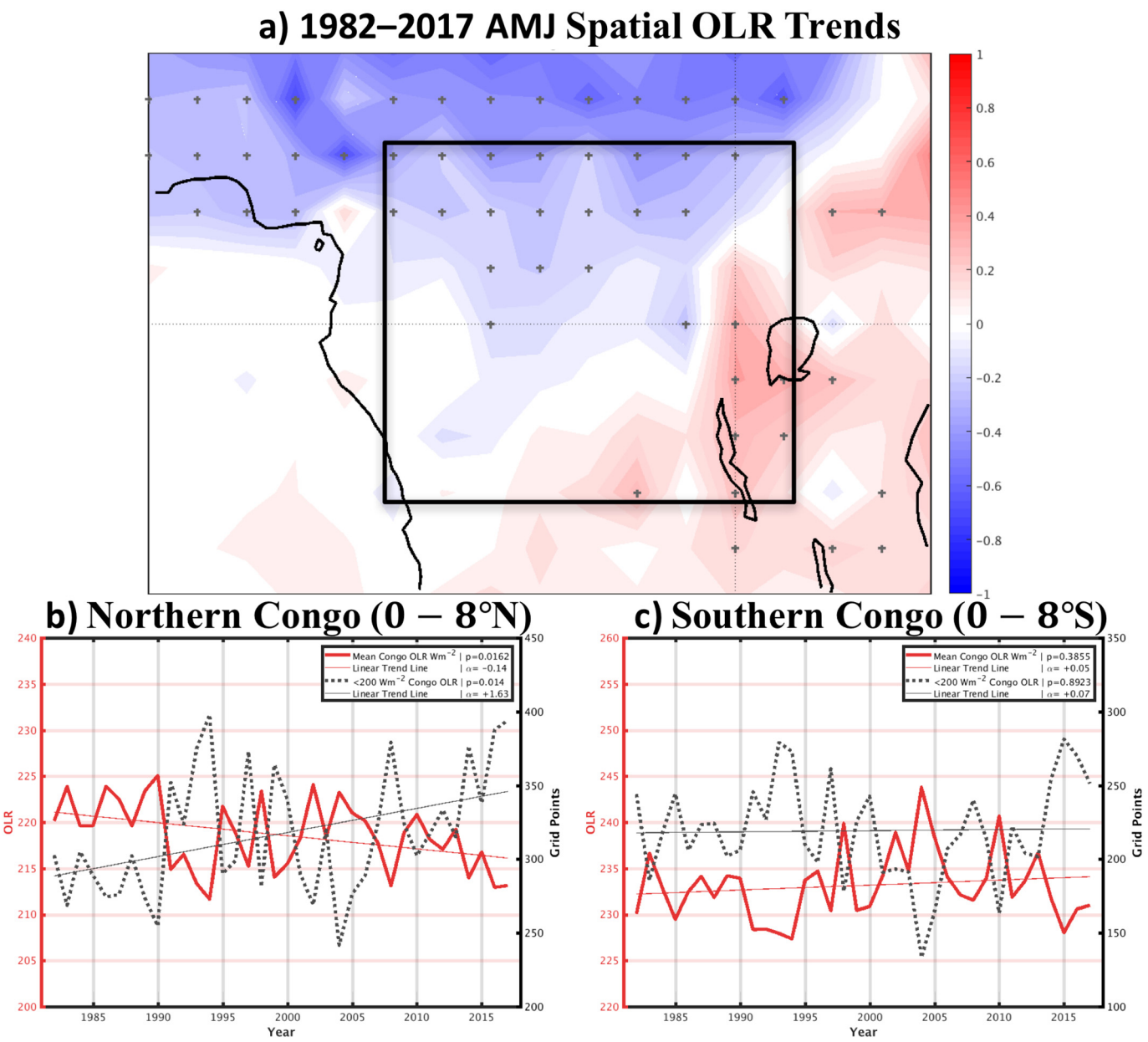

Fig. 5. a) Trends in AMJ OLR (shaded in $Wm^{-2}yr^{-1}$) calculated from 1982 to 2017 using interpolated and uninterpolated data provided by the NOAA/OAR/ESRL PSD, Boulder, Colorado, USA (available at https://www.esrl.noaa.gov/psd/). Trends significant at $p < 0.05$ are shown using the '+' symbol. Interannual variations in the reginal mean OLR (red curve; left axis) and the daily mean number of pixels (right axis) for OLR < 200 Wm^{-2} are shown for b) Northern Congo, and c) Southern Congo. The linear trend (∝) and its *p*-value (p) are shown in this panel. Note: The uninterpolated OLR data was interpolated following the techniques highlighted in Liebmann and Smith (1996) prior to being analyzed. (For interpretation of the references to colour in this figure legend, the reader is referred to the web version of this article.)

cell embedded in such an environment may reach higher heights (i.e., more intense thunderstorms) attributed to the vertical advection of a parcel by the environment. We illustrate the above hypothesis in Fig. 4 where we observed an increase in thunderstorm intensity along the AMJ climatological center of the ITCZ, and a decrease in thunderstorm intensity south of the ITCZ. The Congo has been experiencing accelerated drought whereas the Sahel has become greener due to the recent increase in surface precipitation (Taylor et al., 2017). This result suggests that an increase in thunderstorms activity may not result in a corresponding increase in surface precipitation.

As previously stated, the precipitation climatology and trend over the Congo poses fascinating questions involving many interconnected processes (e.g., ITCZ, SSTs, thunderstorms, and Walker circulation) across different spatiotemporal scales of motion, and we often find it difficult to decouple and isolate a single mechanism that may explain most of the observed rainfall trend. Therefore, future work is necessary to understanding physical mechanisms (e.g., water cycle and moisture budget, and cloud microphysics) responsible for the observed trends in thunderstorm activity presented in this paper using both idealized and fully coupled numerical modeling experiments. Also, more work is needed to investigate trends in the lifecycle and duration of thunderstorms over the Congo, which will be of interest to better understand trends in precipitation frequency, intensity, and duration over the Congo.

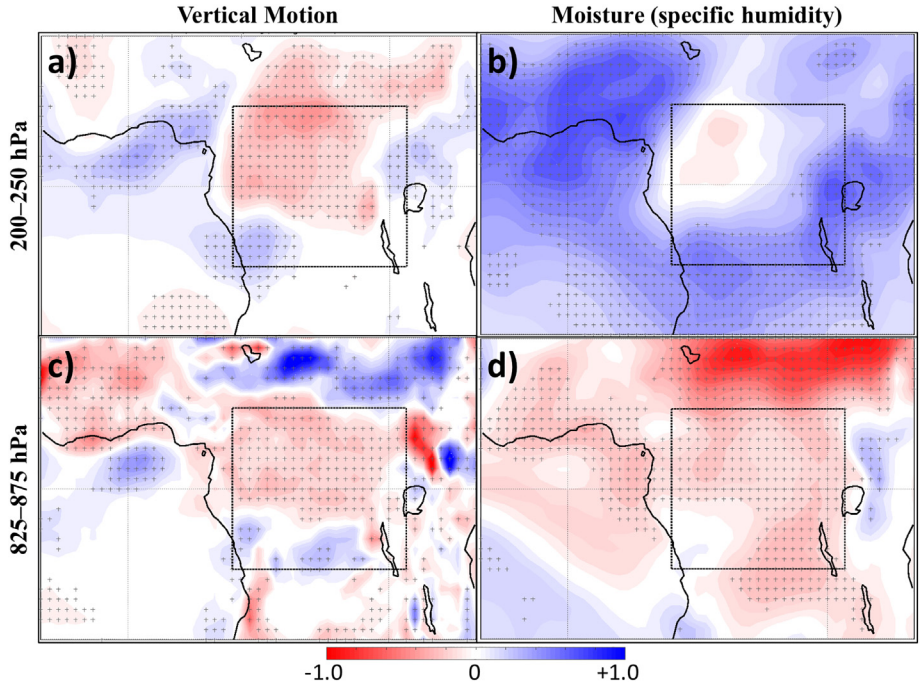

Fig. 6. Trends in AMJ vertical velocity (shaded in $\times\ ^{-1}/_{4}$Pa s^{-1}yr^{-1}) for (a) 200–250 hPa and (c) 875–825 hPa, and trends in AMJ specific humidity for (b) 200–250 hPa ($\times 10^{-3}$ g kg^{-1}yr^{-1}) and (d) 875–825 hPa (g kg^{-1}yr^{-1}) calculated from ERA-Interim. Trends significant at $p < 0.05$ are shown using the '+' symbol.

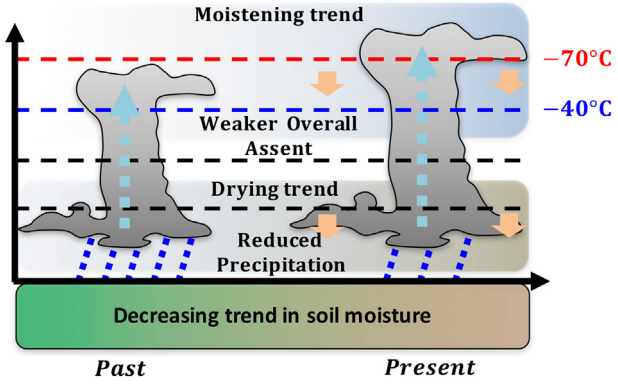

Fig. 7. An illustration of changes observed over the Congo from 1982 to 2016. Trends include larger and more intense thunderstorms over Northern Congo, increase (decrease) in the mean size of thunderstorm at lower (higher) T_b, a drier (wetter) lower (upper) troposphere, and weaker ascent at both the lower and upper troposphere, and an overall reduction in soil moisture. These changes were found to be associated with a significant decrease in AMJ precipitation over the Congo during the same period.

Acknowledgements

This work was supported by the National Science Foundation (NSF AGS-1535426). We would like to thank Dr. Kenneth R. Knapp (NOAA/NCEI) for his expert knowledge and assistance in helping us better understand the GridSat-B1 dataset. We are grateful for the constructive comments and feedback from two anonymous reviewers that helped us improve the quality of this paper.

References

Asefi-Najafabady, S., Saatchi, S., 2013. Response of African humid tropical forests to recent rainfall anomalies. Philos. Trans. R. Soc. B 368, 20120306.
Byrne, M.P., Schneider, T., 2016. Narrowing of the ITCZ in a warming climate: physical mechanisms. Geophys. Res. Lett. 43, 11350–11357.
Cecil, D.J., Buechler, D.E., Blakeslee, R.J., 2015. TRMM LIS climatology of thunderstorm occurrence and conditional lightning flash rates. J. Clim. 28, 6536–6547.
Dai, A., 2006. Precipitation characteristics in eighteen coupled climate models. J. Clim. 19, 4605–4630.
Dee, D.P., et al., 2011. The ERA-interim reanalysis: configuration and performance of the data assimilation system. Q. J. R. Meteorol. Soc. 137, 553–597.
Dezfuli, A.K., Nicholson, S.E., 2013. The relationship of interannual variability in western equatorial Africa to the tropical oceans and atmospheric circulation. Part II. The boreal autumn. J. Clim. 26, 66–84.
Dyer, E.L.E., Jones, D.B.A., Nusbaumer, J., Li, H., Collins, O., Vettoretti, G., Noone, D., 2017. Congo Basin precipitation: assessing seasonality, regional interactions, and sources of moisture. J. Geophys. Res. Atmos. 122, 6882–6898.
Fu, R., 2015. Global warming-accelerated drying in the tropics. PNAS 112, 3593–3594.
Futyan, J.M., Del Genio, A.D., 2007. Deep convective system evolution over Africa and the tropical Atlantic. J. Clim. 20, 5041–5060.
Guan, K., et al., 2015. Photosynthetic seasonality of global tropical forests constrained by hydroclimate. Nat. Geosci. 8, 284–289.
Harris, N.L., et al., 2017. Using spatial statistics to identify emerging hot spots of forest loss. Environ. Res. Lett. 12, L024012.
Hodges, K.I., Thorncroft, C.D., 1997. Distribution and statistics of African mesoscale convective weather systems based on the ISCCP Meteosat imagery. Mon. Weather Rev. 125, 2821–2837.
Hodges, K.I., Chappell, D.W., Robinson, G.J., Yang, G., 2000. An improved algorithm for generating global window bright- ness temperatures from multiple satellite infrared imagery. J. Atmos. Ocean. Technol. 17, 1296–1312.
Hua, W., Zhou, L., Chen, H., Nicholson, S.E., Raghavendra, A., Jiang, Y., 2016. Possible causes of the central equatorial African long-term drought. Environ. Res. Lett. 11, L124002.
Hua, W., Zhou, L., Chen, H., Nicholson, S.E., Jiang, Y., Raghavendra, A., 2018. Understanding the Central Equatorial African long-term drought using AMIP-type simulations. Clim. Dyn. 50, 1115–1128.
Hung, M.-P., Lin, J.-L., Wang, W., Kim, D., Shinoda, T., Weaver, S.J., 2013. MJO and convectively coupled equatorial waves simulated by CMIP5 climate models. J. Climate 26, 6185–6214.
Jiang, Y., Zhou, L., Hua, W., Raghavendra, A., 2018. Increased in dry season length over the Congo, 31st conference on climate variability and change, Austin, TX. Amer. Meteor. Soc. 954. https://ams.confex.com/ams/98Annual/webprogram/Paper328387.html.
Joyce, R., Janowiak, J., Huffman, G., 2001. Latitudinally and seasonally dependent zenith-angle corrections for geostationary satellite IR brightness temperatures. J. Appl. Meteorol. 40, 689–703.
Kawase, H., Abe, M., Yamada, Y., Takemura, T., Yokohata, T., Nozawa, T., 2010. Physical mechanism of long-term drying trend over tropical North Africa. Geophys. Res. Lett. 37, L09706.
Knapp, K.R., 2008. Scientific data stewardship of international satellite cloud climatology project B1 global geostationary observations. J. Appl. Remote. Sens. 2, 023548.
Knapp, K.R., 2012. Intersatellite bias of the high-resolution infrared radiation sounder water vapor channel determined using ISCCP B1 data. J. Appl. Remote. Sens. 6, 063523.
Knapp, K.R., et al., 2011. Globally gridded satellite (GridSat) observations for climate studies. Bull. Amer. Meteor. Soc. 92, 893–907.

Laing, A.G., Fritsch, J.M., 1993. Mesoscale convective complexes in Africa. Mon. Weather Rev. 121, 2254–2263.
Lee, H.-T., Schreck, C.J., Knapp, K.R., 2014. Generation of the daily OLR climate data record. In: 2014 EUMETSAT Meteorological Satellite Conference, 22–26 September 2014, (Geneva, Switzerland).
Lewis, S.L., 2006. Tropical forests and the changing earth system. Philos. Trans. R. Soc. Lond. B 361, 195–210.
Lewis, S.L., et al., 2009. Increasing carbon storage in intact African tropical forests. Nature 457, 1003–1006.
Liebmann, B., Smith, C.A., 1996. Description of a complete (interpolated) outgoing longwave radiation dataset. Bull. Amer. Metor. Soc. 77, 1275–1277.
Maidment, R.I., Grimes, D., Allan, R.P., Tarnavsky, E., Stringer, M., Hewison, T., Roebeling, R., Black, E., 2014. The30 year TAMSAT African RainfallClimatology and time series (TARCAT) dataset. J. Geophys. Res. Atmos. 119, 10619–10644.
Maidment, R.I., Allan, R.P., Black, E., 2015. Recent observed and simulated changes in precipitation over Africa. Geophys. Res. Lett. 42, 8155–8164.
Malhi, Y., Wright, J., 2004. Spatial patterns and recent trends in the climate of tropical rainforest regions. Philos. Trans. R. Soc. Lond. B 359, 311–329.
McCollum, J.R., Gruber, A., Ba, M.B., 2000. Discrepancy between gauges and satellite estimates of rainfall in equatorial Africa. J. Appl. Meteorol. 39, 666–679.
Mildrexler, D.J., Zhao, M., Running, S.W., 2011. A global comparison between station air temperatures and MODIS land surface temperatures reveals the cooling role of forests. J. Geophys. Res. 116, G03025.
Muller, C., Bony, S., 2015. What favors convective aggregation and why? Geophys. Res. Lett. 42, 5626–5634.
National Research Council (NRC), 2004. Climate Data Records from Environmental Satellites. vol. 150 National Academies Press, Washington, DC.
Nesbitt, S.W., Zipser, E.J., 2003. The diurnal cycle of rainfall and convective intensity according to three years of TRMM measurements. J. Clim. 16, 1456–1475.
Niang, I., Ruppel, O.C., Abdrabo, M.A., et al., 2014. Climate Change 2014: Impacts, Adaptation, and Vulnerability. In: Barros, V.R., Field, C.B., Dokken, D.J. (Eds.), Part B: Regional Aspects. Contribution of Working Group II to the Fifth Assessment Report of the Intergovernmental Panel on Climate Change. Cambridge University Press, Cambridge, United Kingdom and New York, NY, USA, pp. 1199–1265.
Nicholson, S.E., 2014. Spatial teleconnections in African rainfall: a comparison of 19th and 20th century patterns. The Holocene 24, 1840–1848.
Nicholson, S.E., Dezfuli, A.K., 2013. The relationship of interannual variability in western equatorial Africa to the tropical oceans and atmospheric circulation. Part I. The boreal spring. J. Clim. 26, 45–65.
Nicholson, S.E., Fink, A.H., Funk, C.C., Vaughan, T.A., 2018. Re-examining the ITCZ as a control on rainfall and its variability in equatorial Africa. 31st conference on climate variability and change, Austin, TX, Amer. Meteor. Soc. 10A, 6. https://ams.confex.com/ams/98Annual/webprogram/Paper323550.html.
Petersen, W.A., Rutledge, S.A., 2001. Regional variability in tropical convection: observations from TRMM. J. Clim. 14, 3566–3586.
Pokam, W.M., Djiotang, L.A.T., Mkankam, F.K., 2012. Atmospheric water vapor transport and recycling in equatorial Central Africa through NCEP/NCAR reanalysis data. Clim. Dyn. 38, 1715–1729.
Raghavendra, A., Guinn, T.A., 2016. Breakdown of ITCZ-like PV Patterns. Beyond: Undergrad. Res. J., 1 1–11.
Sassen, K., Krueger, S.K., 1993. Toward an empirical definition of virga: comments on “is virga rain that evaporates before reaching the ground?”. Mon. Weather Rev. 121, 2426–2428.
Schiffer, R.A., Rossow, W.B., 1983. The international satellite cloud climatology project (ISCCP): the first project of the world climate research Programme. Bull. Amer. Meteor. Soc. 64, 779–784.
Schmetz, J., Tjemkes, S.A., Gube, M., van de Berg, L., 1997. Monitoring deep convection and convective overshooting with METEOSAT. Adv. Space Res. 19, 433–441.
Schroeder, S.R., McGuirk, J.P., 1998. Widespread tropical atmospheric drying from 1979 to 1995. Geophys. Res. Lett. 25, 1301–1304.
Soden, B.J., Jackson, D.L., Ramaswamy, V., Schwarzkopf, M.D., Huang, X., 2005. The radiative signature of upper tropospheric moistening. Science 310, 841–844.
Soula, S., Kasereka, J.K., Georgi, J.F., Barthe, C., 2016. Lightning climatology in the Congo Basin. Atmos. Res. 178-179, 304–319.
Su, H., et al., 2017. Tightening of tropical ascent and high clouds key to precipitation change in a warmer climate. Nat. Commun. 8, 15771.
Taylor, C.M., et al., 2017. Frequency of extreme Sahelian storms tripled since 1982 in satellite observations. Nature 544, 475–478.
Washington, R., James, R., Pearce, H., Pokam, W.M., Moufouma-Okia, W., 2013. Congo Basin rainfall climatology: can we believe the climate models? Philos. Trans. R. Soc. Lond. B 368, 20120296.
Yang, G.Y., Slingo, J., 2001. The diurnal cycle in the tropics. Mon. Weather Rev. 129, 784–801.
Zhou, L., et al., 2014. Widespread decline of Congo rainforest greenness in the past decade. Nature 509, 86–90.
Zipser, E.J., Cecil, D.J., Liu, C., Nesbitt, S.W., Yorty, D.P., 2006. Where are the most intense thunderstorms on earth? Bull. Amer. Meteor. Soc. 87, 1057–1071.